



**HAL**  
open science

## Theoretical and experimental study of ScAlN/Sapphire structure based SAW sensor

F. Bartoli, Thierry Aubert, M. Moutaouekkil, J. Streque, P. Pigeat, S. Hage-Ali, P. Boulet, H. M'Jahed, Olivier Bou Matar, Abdelkrim Talbi, et al.

► **To cite this version:**

F. Bartoli, Thierry Aubert, M. Moutaouekkil, J. Streque, P. Pigeat, et al.. Theoretical and experimental study of ScAlN/Sapphire structure based SAW sensor. 2017 IEEE SENSORS, Oct 2017, Glasgow, United Kingdom. 10.1109/ICSENS.2017.8233938 . hal-01692287

**HAL Id: hal-01692287**

**<https://hal.science/hal-01692287>**

Submitted on 24 Jan 2018

**HAL** is a multi-disciplinary open access archive for the deposit and dissemination of scientific research documents, whether they are published or not. The documents may come from teaching and research institutions in France or abroad, or from public or private research centers.

L'archive ouverte pluridisciplinaire **HAL**, est destinée au dépôt et à la diffusion de documents scientifiques de niveau recherche, publiés ou non, émanant des établissements d'enseignement et de recherche français ou étrangers, des laboratoires publics ou privés.

# Theoretical and experimental study of ScAlN/Sapphire structure based SAW sensor

F. Bartoli, M. Moutaouekkil, J. Streque, P. Pigeat,  
S. Hage-Ali, P. Boulet, H. M'Jahed and O. Elmazria,  
Institut Jean Lamour UMR 7198  
Université de Lorraine - CNRS  
54506 Vandœuvre-lès-Nancy, France

F. Bartoli, T. Aubert  
LMOPS EA 4423  
CentraleSupélec - Université de Lorraine  
57070 Metz, France

Sergei Zhgoon  
National Research University "MPEI"  
14, Krasnokazarmennaya  
121351, Moscow Russia

O. Bou Matar, A. Talbi  
Joint International Laboratory LIA LICS  
Univ. Lille, CNRS, Centrale Lille, ISEN, Univ.  
Valenciennes, UMR 8520 - IEMN  
59651 Villeneuve d'Ascq, France

**Abstract** — Several SAW devices based on  $\text{Sc}_{0.1}\text{Al}_{0.9}\text{N/Sapphire}$  bilayer structures were fabricated using various wavelengths and film thicknesses. The acoustic velocity, electromechanical coupling coefficient and temperature coefficient of frequency (TCF) of each device was then measured and the results were compared with calculations using several sets of elastic, piezoelectric and dielectric constants available in the literature. We have shown that the accuracy of available constants is not enough to permit a reliable optimization and design of SAW devices for signal processing and sensors applications.

**Keywords**—Temperature sensor, SAW, ScAlN

## I. INTRODUCTION

Thanks to its high acoustic phase velocity, low motional resistance, high thermal conductivity, and CMOS-compatibility [1,2], AlN thin films have attracted attention as piezoelectric material for RF-MEMS including bulk and surface acoustic wave devices. Moreover, AlN is chemically inert and shows a high temperature stability. Indeed it is an intrinsically-poled, non-ferroelectric material (no Curie point) which has been reported to retain its piezoelectric properties at temperatures above 1000°C [3]. However, the low electromechanical coupling coefficient ( $K^2$ ) and piezoelectric constant ( $d_{33}$ ) of AlN thin compared to PZT and ZnO thin films, limits its wide applications in sensors, wide band filters, and MEMS including for energy harvesting.

Recently, several studies have shown that the addition of Sc to form  $\text{Sc}_x\text{Al}_{1-x}\text{N}$  strongly increases the measured piezoelectric coefficients of ScAlN alloys, until reaching a phase transition to the non-polar rocksalt-type structure [1,2] ( $x=0.43$ ). It was reported that an enhancement of 400% of  $d_{33}$  is obtained for  $\text{Sc}_{0.43}\text{Al}_{0.57}\text{N}$  alloys compared to pure AlN [4]. Moreover, the ScAlN has all the advantages of the AlN mentioned below. Because of its strong electromechanical coupling and improved piezoelectricity, ScAlN allows to widen the field of applications and especially that of sensors. Note also that the expected energy harvesting factor of merit ( $FOM = \frac{e_{31}^2}{\epsilon_0 \epsilon_r}$ ) for  $\text{Sc}_{0.43}\text{Al}_{0.57}\text{N}$  (60GPa) is larger than those of PZT (24GPa) or ZnO (10.8GPa) [5].

The aim of this work is to develop a wireless, batteryless and packageless acoustic wave sensor based on the three layers structure AlN/ScAlN/Sapphire. In order to develop fully operational sensors and optimize their design according to the targeted performance, the full and accurate physical constants of the materials considered are a prerequisite. If these constants are now well established for Sapphire and AlN, it is not the case for ScAlN. Several sets of constants could be found in literature [7-11] and these constants are of course depending on the concentration of scandium in the film. These constants, determined by different experimental methods or by calculation, show a strong scatter, making the choice of the accurate set difficult. Consequently, and in order to determine the most suitable set of constants, we first studied the bilayer structure ScAlN/Sapphire and compared experimental results with calculated ones. The selected set is then used to optimize the whole set constants AlN/ScAlN/Sapphire structure.

## II. MODELING DETAILS AND METHOD

Phase velocity of ScAlN/Sapphire structures have been determined using the recently reported Legendre and Laguerre polynomial approach of wave propagation in layered magneto-electro-elastic structures by which is a flexible and computationally efficient alternative to the classical solution of transcendental equations [12]. For  $S_{11}$  coefficient calculation, a numerical model in Comsol Multiphysics using general partial derivative equations interface. A half period of an infinite IDT with periodic boundary conditions in the propagation direction is used. Dispersion curves of acoustic velocity were calculated versus ScAlN film thickness, and for various Sc concentration in the film.

Like AlN, ScAlN is part of the family of hexagonal piezoelectric crystals (class 6mm) and can be defined by 10 independent material constants as follows:

Elastic stiffness:  $C_{11}, C_{12}, C_{13}, C_{33}, C_{44}$ , with  $C_{66} = \frac{C_{11} - C_{12}}{2}$

Piezoelectric constants:  $e_{15}, e_{31}, e_{33}$

Dielectric constants:  $\epsilon_{11}, \epsilon_{33}$ ,

To optimize the considered structure and thus the design of acoustic wave devices, the full and accurate material constant

sets are required. Table 1 summarizes the main data collected in published works concerning the ScAlN. It has been demonstrated by calculation [10] and experimentally [9] that the elastic constants  $C_{ij}$  vary linearly with the concentration of

Scandium. In order to obtain a complete set of constants for lower concentrations, we have determined these constants by extrapolation considering those of the pure AlN ( $x = 0\%$ ) and the available ones (generally  $x = 43\%$ ).

TABLE I. PHYSICAL CONSTANTS OF CONSIDERED MATERIAL

Material	Elastic stiffness (GPa)	Piezoelectric constants (C/m <sup>2</sup> )	Dielectric constants	Density (kgm <sup>-3</sup> )	Ref
	$C_{11}, C_{12}, C_{13}, C_{33}, C_{44}, C_{66}$	$e_{15}, e_{31}, e_{33}$	$\epsilon_{11}, \epsilon_{33}$	$\rho$	
AlN	345, 125, 120 395, 118, 110	-0.48, -0.58, 1.55	8, 9.5	3260	[6]
Sc <sub>43%</sub> AlN <sub>57%</sub>	234.5, 101.4, 128.4, 267.4, 39.6, 66.6	1.03, -0.886, 0.863	24.1, 12.3	3601	[7]
	169, 61.2, 58.8, 211, 51.5, 53.9	-1.31, -1.58, 4.42	30.5, 30.28	3760	[8]
	282.4, 136.5, 125.2, 169.6, 98.1, 98.1	-0.294, -0.516, 2.72	30.5, 30.28	3760	[9]
	313.7, 150, 139.2, 197, 108.6, 108.6	-0.317, -0.722, 2.73	30.5, 30.28	3760	[10]
	293, 146, 130, 184, 100, 74.7	-1.31, -1.58, 4.42	30.5, 30.28	3760	[11]

### III. EXPERIMENTAL

#### A. ScAlN deposition

Scandium Aluminum Nitride thin films were deposited by reactive magnetron sputtering. 10% scandium and 18% scandium thin films have been made with single composite Sc/Al targets, respectively composed of 12.5% and 25% of Scandium. The films compositions have been measured by Energy Dispersive X-Ray Spectroscopy (EDXS). Structural properties such as microstructure and nanostructure have been determined by  $\theta$ -2 $\theta$ , rocking-curve and pole figures X-Rays Diffraction (XRD) measurements and by Transmission Electron Microscopy (TEM) measurements. The Sc<sub>0.1</sub>Al<sub>0.9</sub>N and Sc<sub>0.18</sub>Al<sub>0.82</sub>N thin films shows strong (002) orientation, with high texturing which guarantees good piezoelectric properties which in principle enables to obtain good piezoelectric properties.

#### B. SAW devices fabrication

Several SAW devices based on ScAlN/Sapphire bilayer structures were fabricated using photolithography and chemical etching process. SAW devices consist in asynchronous resonator. Aluminum Interdigital transducer (IDT) and reflectors were fabricated by conventional contact ultraviolet (UV) photolithography. Resonators consist in 100 IDT pairs and 200 reflectors on each side. Two spatial periods ( $\lambda = 6.5$  and  $13\mu\text{m}$ ) and three ScAlN thicknesses (1.6, 2.23 and  $2.76\mu\text{m}$ ) were considered. Thus, six values of relative thickness ( $h_{\text{ScAlN}} = h/\lambda$ ) are obtained, leading to plot dispersion curves of velocity,  $K^2$  and temperature coefficient of frequency (TCF).

### IV. RESULTS AND DISCUSSION

As an example, figure 1 shows the wide range frequency response of a SAW resonator fabricated with ( $\lambda = 6.5\mu\text{m}$  and  $h_{\text{ScAlN}} = 2.76\mu\text{m}$ ). We can observe the Rayleigh wave at 729 MHz and its 2<sup>nd</sup> and 3<sup>rd</sup> mode at 1025MHz and 1566MHz. The larger coupling is obtained for the 3<sup>rd</sup> mode ( $K^2 = 1.7\%$ ) while 0.77% and 0.49% were obtained respectively for modes 1 and 2. We note that for lower relative thicknesses of ScAlN, only the mode 1 of Rayleigh wave is generated. In the following part our

study will be focused only on this mode. The phase velocities ( $v$ ) were determined from the resonance frequency  $f_r$  ( $v = \lambda \cdot f_r$ ). The experimental values of  $K^2$  were determined using resonance ( $f_r$ ) and antiresonance ( $f_a$ ) frequencies determined from admittance  $Y$  plot and using formula  $K^2 = 1 - (f_r/f_a)^2$ . All devices were characterized versus temperature leading to determination of TCF values.

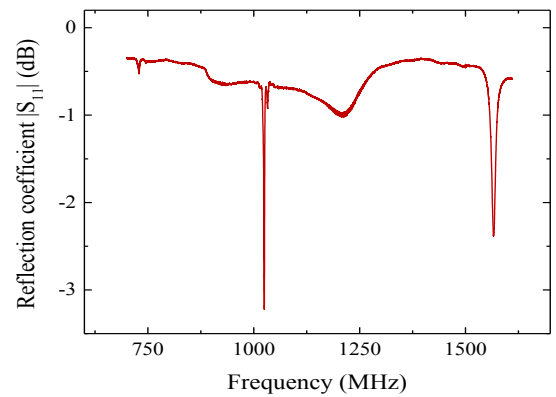


Fig. 1. Frequency response of a AlN/Sapphire SAW resonator fabricated with  $h_{\text{ScAlN}} = 2.76\mu\text{m}$  and  $\lambda = 6.5\mu\text{m}$ .

Figure 2 shows the dispersion curves of the phase velocity for a scandium concentration of 43%. As reference curve, dispersion curves of pure AlN were also plotted in the same graphs. As expected, the calculated values are strongly dependent on the considered set of constants. To determine the most accurate set, we plot in the same graph the experimental value of velocity measured for samples with scandium concentration of 10 % and the calculated velocity values (Fig. 3). One can observe that the measured velocities are lower than the calculated ones regardless of the constant set used. The experimental data are closer to those calculated for 43% of scandium with Zhang set [10]. These differences could be explained by cracks at the surface due to the high temperature deposition of the ScAlN thin film, which could decrease the SAW velocity. Further investigations are made for more informations. If the data published by Konno remains the closest to the experimental ones, they are nevertheless not suitable for making a reliable optimization.

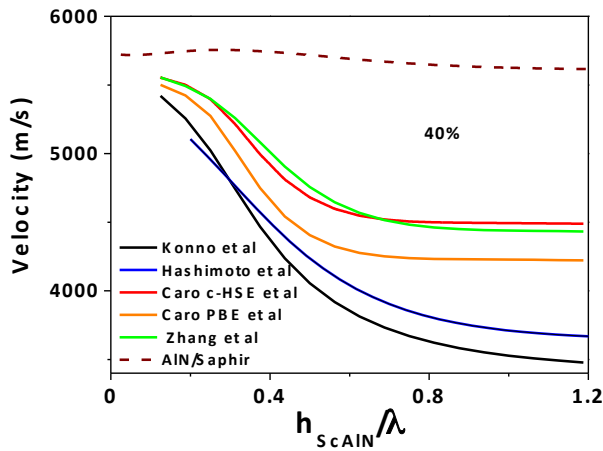


Fig. 2. Dispersion curve of velocity calculated for  $\text{Sc}_{0.43}\text{Al}_{0.57}\text{N}/\text{Sapphire}$  structure using five different sets of physical constants.

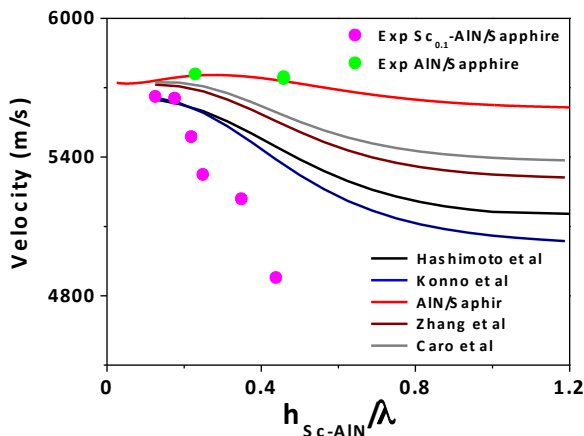


Fig. 3. Dispersion curve of velocity measured and calculated for  $\text{Sc}_{0.1}\text{Al}_{0.9}\text{N}/\text{Sapphire}$  structure.

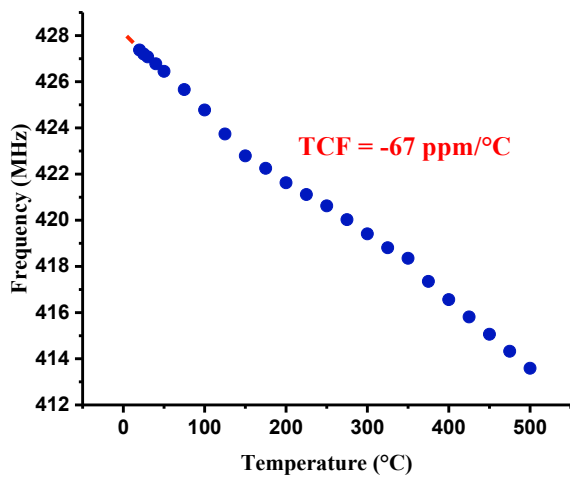


Fig. 4. Measured TCF for a  $2.76 \mu\text{m}$   $\text{ScAlN}$  thin film on Sapphire substrate, with  $\lambda = 13 \mu\text{m}$ .

TCF values were also determined for various devices made with  $\text{Sc}_{0.1}\text{Al}_{0.9}\text{N}$ . These values are depending on both relative film thickness and scandium concentration. For characterized devices the TCF is ranging from  $-110 \text{ ppm}/^\circ\text{C}$  to  $-40 \text{ ppm}/^\circ\text{C}$ . For instance, Figure 4 shows a TCF of  $-67 \text{ ppm}/^\circ\text{C}$ , for temperatures between  $20^\circ\text{C}$  and  $500^\circ\text{C}$ . Therefore, the  $\text{Sc}_{0.1}\text{Al}_{0.9}\text{N}$  shows a good sensitivity of the temperature, and it is able to operate up to  $500^\circ\text{C}$ . Since the IDT were made with aluminum, the robustness of the film to higher temperatures has not been tested yet. Moreover, the advantage of such structure is that the TCF and thus the sensitivity of the temperature sensor, could be adjusted to match application requirements by controlling the film thickness and/or the Sc to Al ratio.

## V. CONCLUSION

Highly textured Scandium Aluminum Nitride thin films were deposited by reactive magnetron sputtering on sapphire substrates. The film quality was demonstrated by XRD and TEM measurements and by the performances of the fabricated SAW resonators. The comparison of the dispersion curves of velocity calculated and determined experimentally, shows a strong divergence thus suggesting the inaccuracy of the physical constants available in the literature for the  $\text{ScAlN}$ . The unavailability of elastic constants thermal properties does not make it possible to determine the TCF of the  $\text{ScAlN}/\text{Sapphire}$  structure by calculation.

## REFERENCES

- [1] M. Akiyama, T. Kamohara, K. Kano, A. Teshigahara, Y. Takeuchi, and N. Kawahara, *Advanced Materials* 21, 593(2009).
- [2] S. Zhang, D. Holec, W. Y. Fu, C. J. Humphreys, and M. A. Moram, *Journal of Applied Physics* 114, 133510 (2013).
- [3] T. Aubert, J. Bardong, O. Legrani, O. Elmazria, M. B. Assouar, G. Bruckner; *J. of Applied Physics*, Vol. 114, art. Nu 014505; (2013)
- [4] M. Akiyama, K. Umeda, A. Honda, and T. Nagase, *Applied Physics Letters* 102, 021915 (2013).
- [5] P. M. Mayrhofer, C. Rehlend, M. Fischeneder, M. Kucera, E. Wistrela, A. Bittner, and U. Schmid; *JOURNAL OF Microelectromechanical Systems*, Vol. 26, pp 102-112, (2017)
- [6] K. Tsubouchi, K. Sugai and N. Mikoshiba, *Proc. IEEE Ultrasonics Symp.*, pp. 375-380, 1981.
- [7] A. Konno, M. Kadota, J. Kushibiki, Y. Ohashi, M. Esashi, Y. Yamamoto, S. Tanaka; 2014 IEEE International Ultrasonics Symposium Proceedings; pp 273-276 (2014).
- [8] Ken-ya Hashimoto, S. Sato, A. Teshigahara, T. Nakamura and K. Kano; *IEEE Transactions on Ultrasonics, Ferroelectrics, and Frequency Control*, vol. 60, no. 3, pp 637 - 642, March (2013).
- [9] M.A. Caro, S. Zhang, M. Ylilampi, T. Riekkinen, M. A Moram, O. Lopez-Acevedo, J. Molarius and T. Laurila; *J. Phys. Condens. Matter* 27 245901; (2015)
- [10] S. Zhang, W. Y. Fu, D. Holec, C. J. Humphreys and M. A. Moram; *Journal of Applied Physics* 114, 243516, pp 1-6 (2013).
- [11] G. Carlotti, J. Sadhu, F. Dumont; *IEEE International Ultrasonics Symposium (IUS)*, 1037, pp 1 (2017).
- [12] O. Bou Matar, N. Gasmı, H. Zhou, M. Goueygou, and A. Talbi, *J. Acoust. Soc. Am.* 133, 1415 (2013)].